Separate activation of fast and slow inhibitory postsynaptic potentials in rat neocortex *in vitro*

L. S. Benardo

Departments of Neurology and Pharmacology, State University of New York Health Science Center at Brooklyn, Brooklyn, NY 11203, USA

1. Synaptic inhibition was investigated by stimulating inhibitory neurones with focal microapplications of glutamate, while recording from layer V pyramidal neurones of rat somatosensory cortical slices.

2. One class of inhibitory postsynaptic potentials (IPSPs) thus elicited was characterized as a fast, chloride-mediated, $GABA_A$ IPSP in part by its fast time-to-peak (mean 2·5 ms) and brief duration, but primarily on the basis of its reversal potential at −68 mV, and its blockade by picrotoxin.

3. The average peak amplitude for these fast IPSPs was −1·5 mV, measured at −60 mV. The peak conductance calculated for these events was about 10 nS.

4. The conductance change associated with the maximal fast inhibitory postsynaptic potential resulting from electrical stimulation of afferent pathways ranged up to 116 nS.

5. A second class of IPSP was encountered much less frequently. These glutamate-triggered events were characterized as slow, potassium-mediated $GABA_B$ IPSPs partly because of their longer times-to-peak (mean, 45 ms) and duration, but especially because of their extrapolated equilibrium potential at about −89 mV and blockade by 2-hydroxysaclofen.

6. The average peak amplitude for these slow IPSPs was −2·3 mV, measured at −60 mV. The peak conductance for these events was about 8 nS.

7. IPSPs resulting from the excitation of individual inhibitory interneurones were elicited by glutamate microapplication at particular locations relative to recording sites. Both fast and slow IPSPs were generated, but these occurred as separate events, and mixed responses were never seen.

8. Thus, the two mechanistically distinct types of IPSPs which result from GABA interaction at $GABA_A$ and $GABA_B$ receptors on neocortical neurones may be mediated by separate classes of inhibitory neurones.

Inhibition is pivotal in the integration of all activity within the neocortex. This occurs because neuronal excitability in the cortex is regulated by the balance between excitatory and inhibitory influences (Traub & Wong, 1982; Chagnac-Amitai & Connors, 1989; Miles, 1990; Benardo & Wong, 1994). In the task of normal information processing, inhibition functions in shaping and directing the flow of excitatory signals. In addition, inhibition maintains synaptic stability. Reducing inhibition releases hyperexcitability and quickly leads to epileptogenesis sustained by local recurrent excitatory synapses (Miles & Wong, 1986; Chagnac-Amitai & Connors, 1989).

In neocortex, inhibition is mediated primarily by GABA, and is comprised of two types of inhibitory postsynaptic potentials (IPSPs), designated fast and slow (Connors, Gutnick & Prince, 1982; Avoli, 1986; Connors, Malenka & Silva, 1988; Deisz & Prince, 1989). The pharmacology of these two forms of neocortical GABAergic inhibition has been described (Connors *et al.* 1988; Deisz & Prince, 1989). As in hippocampus (Alger, 1991), there are two general classes of GABA receptors, $GABA_A$ and $GABA_B$, that mediate bicuculline-sensitive and -insensitive responses, respectively (Connors *et al.* 1982, 1988; Krnjevic, 1984; Avoli, 1986; Deisz & Prince, 1989; McCormick, 1989). GABA activates both kinds of receptors. The $GABA_A$ response is chloride dependent, and mediates the ligand-gated fast IPSP (Kelly, Krnjevic, Morris & Yim, 1969; Avoli, 1986; Connors *et al.* 1988; Deisz & Prince, 1989; McCormick, 1989). $GABA_B$ receptors activate a postsynaptic potassium-dependent conductance via a G protein-linked mechanism, and hyperpolarize cells (Avoli, 1986; Howe, Sutor & Zieglgansberger, 1987; Connors *et al.* 1988; Deisz & Prince, 1989; McCormick, 1989). Activation of the $GABA_B$ receptor by synaptically released GABA causes the late, slow IPSP.

Despite this knowledge, the physiological details of the inhibitory circuit in neocortex remain unknown. For

example, the fundamental issue of whether or not a single GABAergic interneurone activates both postsynaptic $GABA_A$ and $GABA_B$ receptors has not been explored in neocortex. Technical limitations have largely precluded the detailed physiological examination of neocortical local inhibitory connections required to address these issues.

Dual intracellular recordings provide the most rigorous assessment of local inhibitory circuits. In this manner a single interneurone is stimulated to fire action potentials, and a second principal neurone recorded to detect evoked IPSPs. Direct evidence for recurrent synaptic inhibition has been obtained in CA1 and CA3 of hippocampus using this method (Knowles & Schwartzkroin, 1981; Miles & Wong, 1984; Lacaille, Mueller, Kunkel & Schwartzkroin, 1987). However, securing these types of dual intracellular recordings is technically difficult. Moreover, even with the anatomically favourable conditions provided by the hippocampus, where such local circuits have been studied best, they are sparse (i.e. 2–7 % of cell pairs). The more complicated organization of neocortex would seem to provide an even greater challenge to this approach.

Another technique for investigating local synaptic circuits involves stimulating local neurones with substances such as glutamate. This method has been used to study local inhibitory synaptic inputs to spinal motoneurones (Jankowska & Roberts, 1972; Brink, Harrison, Jankowska, McCrea & Skoog, 1983), cerebellar Purkinje cells (Curtis & Crawford, 1965; Crawford, Curtis, Voorhoeve & Wilson, 1966; Curtis & Felix, 1971), hippocampal pyramidal neurones (Williams & Lacaille, 1992), and neocortical pyramidal cells (Biscoe & Curtis, 1967; Curtis & Felix, 1971; Renaud & Kelly, 1974). Glutamate appears to be specific for soma–dendritic membranes, and not axons of passage (Yamamoto, 1982; Christian & Dudek, 1988), thereby providing an effective method for studying intracortical synaptic circuits independent of projected inputs (Tasker, Peacock & Dudek, 1992). I used glutamate microapplication to study local inhibitory circuits involving layer V neurones in slices of rat somatosensory cortex. The results show that glutamate microdelivery at selected sites can elicit either fast or slow IPSPs, but not mixed events, in postsynaptic pyramidal neurones. The findings also suggest that the different IPSPs triggered arise from the excitation of separate classes of inhibitory interneurones.

METHODS

General

The methods employed were similar to those previously described (Benardo, 1991, 1993*a*). Following halothane anaesthesia, Sprague–Dawley rats (80–100 g) were decapitated, their brains rapidly removed and placed in ice-cold Ringer solution. Slice preparations included the dorsal portion of both hemispheres connected by an intact corpus callosum. To prepare such slices, lateral portions of the cerebral hemispheres were first removed with bilateral parasagittal cuts. The brainstem and anterior portions were then excised. Finally a rostro-caudal horizontal cut through the striatum and the septal nuclei was made. Slices 400 μm thick were obtained, including bilateral cingulate and somatosensory cortices. Slices were cut normal to the sagittal sinus to insure standardization, and care was taken that the bilateral extent of slices was anatomically comparable across preparations.

Slices were placed in a recording chamber and maintained at $35{\cdot}5 \pm 1$ °C. The chamber consisted of an inner part where slices rested on a nylon net, and was of an interface design. Accordingly, slices were bathed from below with warmed Ringer solution saturated with 95 % O_2–5 % CO_2, and warm, moist oxygenated air originating from the chamber's outer jacket flowed over them. Perfusion was constant at approximately 1 ml min^{-1} with waste solution being taken up by suction. The composition of the Ringer solution was (mM): NaCl, 124; KCl, 5; $MgCl_2$, 1·6; $CaCl_2$, 2; $NaCO_3$, 26; glucose, 10. The pH was between 7·35 and 7·4.

Electrophysiological techniques

Recordings were obtained with microelectrodes pulled from 1 mm thin-walled, fibre-filled capillary tubing (WPI, Sarasota, FL, USA) using a Flaming–Brown micropipette puller (P-87, Sutter Instruments, Novato, CA, USA). These unbevelled electrodes were filled with 2 M potassium acetate, or 1 M KCl (pH adjusted to 7·2) and had resistances of 20–60 MΩ. Use of KCl-filled electrodes was limited to those experiments defining slow IPSPs, as noted in the text. Membrane potentials were measured using an amplifier (Axoclamp 2A, Axon Instruments, Foster City, CA, USA) operated in current clamp mode. Slices were stimulated extracellularly with sharpened bipolar, coated tungsten electrodes placed in the deep grey matter lateral to the recording site. Single cathodal shocks of 200 μs duration were delivered through a digitally controlled stimulus isolation unit (WPI). Voltage and current signals were amplified and stored on VHS tape via a digitizing board (Neurodata Instruments, New York), and/or a microcomputer for later off-line analysis which included the use of pCLAMP software (Axon Instruments).

Glutamate microapplication

Pipettes identical to those used for standard intracellular recording were first filled with solutions containing glutamate (2·5–5 mM) by capillary action, then backfilled. Pipettes were fitted into rigid, sealed holders attached to a micromanipulator (Narishige, Tokyo, Japan). Under the visual control of a dissecting microscope at × 20–30, these pipettes were broken back to a tip diameter of 1–2 μm with fine Dumont forceps. A rapidly switching solenoid valve (General Valve, Inc., Fairfield, NJ, USA; response time, 2 ms) was controlled via a digital stimulator (WPI)-activated power supply (Valve Driver, General Valve, Inc.), to gate pulses of compressed air (10 lbf in^{-2}) for precise periods of 2–200 ms. This method has proved reliable for use on intracellularly recorded neurones (Yamamoto, 1982; Connors, 1984; Christian & Dudek, 1988; Tasker *et al.* 1992), and gives reproducible responses with no significant mechanical artifacts, judged by control experiments with saline-filled micropipettes. The amount of substance delivered was linear with pulse duration, and quantifiable by measuring the size of the droplet released in air or under oil. For the typical application of 20 ms the ejected volume was calculated to be less than 1 pl (McCormick, 1989).

To suppress polysynaptic excitation, the excitatory amino acid antagonists 6-cyano-7-nitroquinoxaline-2,3-dione (CNQX) and 3-(2-carboxypiperazine-4-yl)propyl-1-phosphonic acid

(CPP, both from Tocris Neuramin, Bristol, UK) were applied in the bathing medium at 5–10 μM. These concentrations of drugs are effective in blocking excitatory postsynaptic potentials (EPSPs) evoked by single electrical stimuli (Benardo, 1993*a*). But since these are competitive antagonists (Watkins & Olverman, 1987; Drejer & Honore, 1988), focal application of glutamate at the concentrations utilized and with proper localization, overcame blockade causing restricted excitation of select neurones. In practice the glutamate micropipette was brought into the proximity of the intracellular recording electrode, and the thickness of the slice probed for sites eliciting IPSPs in the recorded layer V cell. At successive trial depths a 10–20 ms application of the drug was delivered to test for presynaptic inhibitory sites. Responses to applications of this duration insured close proximity of the glutamate pipette to the excited cell (radius of the sphere of excitation, 25–50 μm, judged by the distance the pipette could be moved before the response declined). As the glutamate pipette was moved through the tissue, intermittent (direct) excitation was recorded in a cell only when glutamate delivery could be effected at locations < 200 μm medial or lateral to the recording site (approximately the breadth of its dendritic tree).

IPSPs could be elicited when the pipette was located at selected locations within a 200 μm radius of the recording site. Cells were routinely maintained at a membrane potential of -60 mV (on average 5–10 mV depolarized to rest potential) so that hyperpolarizing IPSPs would be more easily seen. When an inhibitory response was encountered, the response was optimized by adjusting the glutamate pipette depth by moving the pipette so that the shortest latency IPSP was triggered by the briefest possible drug ejection period. Occasionally, slowly developing, gradual depolarizations mixed with phasic hyperpolarizing responses were encountered, but perseverance in properly locating the drug electrode depthwise allowed IPSPs to be recorded in isolation. These depolarizations were presumably due to direct excitation of the recorded cell by the glutamate application (blockade overcome) onto its dendrites, as noted above. If no inhibitory response was seen at one location, the glutamate pipette was moved. This procedure could be repeated at different sites around a cell, to identify multiple areas eliciting inhibition. Often a fluorescent dye was included in the glutamate pipette for later identification of sites giving rise to IPSPs.

Data throughout this report are expressed as means $\pm$ S.D.

RESULTS

This report is based on recordings from sixty-five layer V neurones of rat somatosensory cortical slices. The mean slope resistance determined from plots of the current–voltage relationship was $24{\cdot}1 \pm 4{\cdot}7$ MΩ, and the mean resting membrane potential was $-68{\cdot}2 \pm 5{\cdot}2$ mV in a representative group of these neurones ($n = 46$). All cells had the characteristics typical for neocortical regular-spiking pyramidal neurones (McCormick, Connors, Lighthall & Prince, 1985).

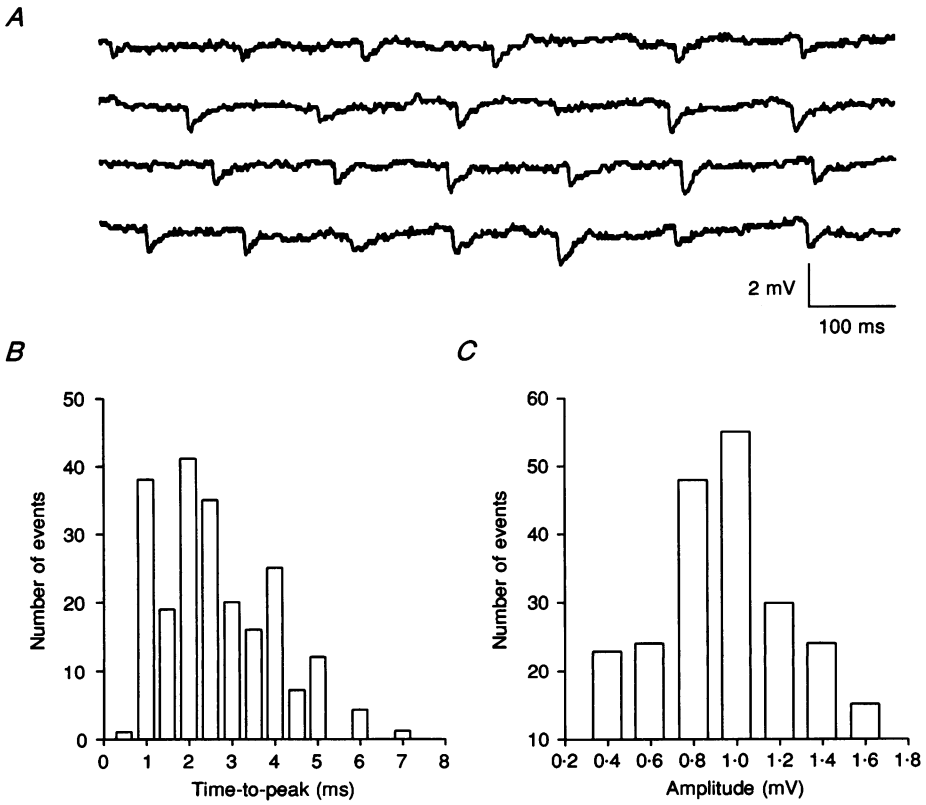

Figure 1. Spontaneous fast hyperpolarizing potentials recorded in a layer V neurone
A, records of spontaneous synaptic activity recorded from a layer V neurone. *B*, distribution of times-to-peak of 219 inhibitory events (mean, $2{\cdot}6 \pm 1{\cdot}3$ ms). *C*, distribution of amplitude of these events (mean, $-1{\cdot}0 \pm 0{\cdot}3$ mV). Measurements were made of synaptic events greater than $-0{\cdot}4$ mV, but only when they occurred after any previous event had already decayed. The resting potential of this neurone was maintained at -60 mV.

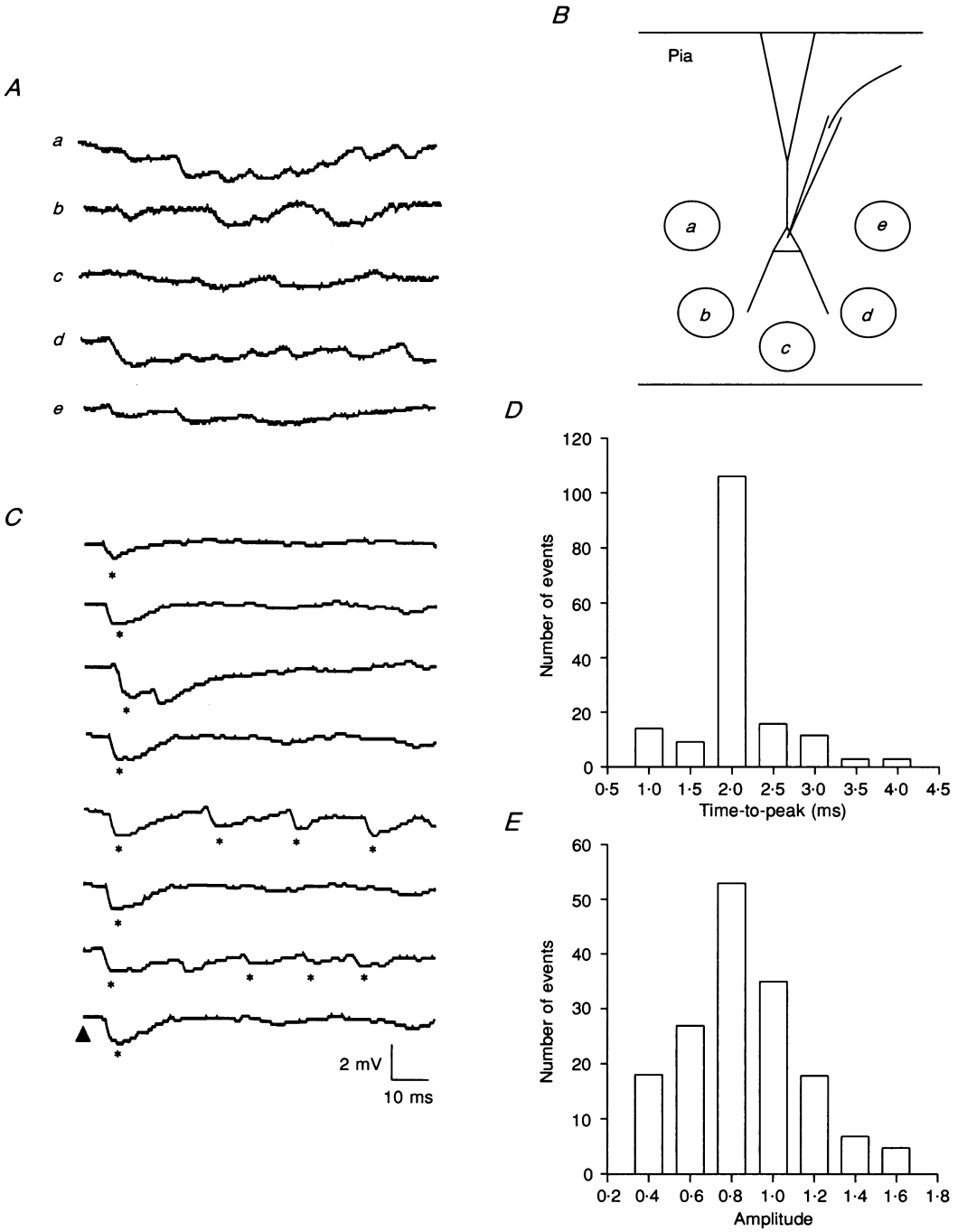

Figure 2. Fast IPSPs triggered in layer V neurones by glutamate microapplication
A, examples of fast IPSPs triggered in a cell by glutamate microapplication (5 mM) in the presence of CNQX (5 μM) and CPP (10 μM) at five different sites, shown schematically in *B* (responses *a–e* in *A* obtained at sites *a–e*, respectively, in *B*). All sites giving rise to fast IPSPs were within 200 μm of the recording site. *C*, eight responses in a single cell to equivalent glutamate microapplications to a single site under the same conditions as in *A*. The triangle marks the offset of a 10 ms application of 2·5 mM glutamate. Throughout, measurements were made of synaptic events greater than −0·4 mV which were non-overlapping. Events included in measurements are marked with an asterisk. *D*, distribution of times-to-peak of 162 IPSPs triggered from a single site in this same cell (mean, 2·1 ± 0·6 ms). *E*, distribution of amplitude of these IPSPs (mean, −0·9 ± 0·3 mV). The resting potential of this neurone was maintained at −60 mV.

Properties of fast inhibitory synaptic potentials

Spontaneous hyperpolarizing potentials such as those shown in Fig. 1*A* could be seen in most neocortical neurones recorded under control conditions. These events were most prominent at potentials somewhat depolarized from the usual resting membrane potential of these cells (as given above), and appeared to reverse in polarity when the membrane potential was maintained at levels more negative than the typical resting potential. Moreover, these potentials were never observed in the presence of the $GABA_A$ antagonist picrotoxin (50 μM; $n = 10$), nor were spontaneous slow IPSPs revealed by this procedure. Addition of tetrodotoxin (1 $\mu g\ ml^{-1}$) to the bath did cause the larger amplitude hyperpolarizing potentials to disappear, and remaining IPSPs appeared less frequently, but this was not quantified further. Therefore, spontaneous IPSPs recorded under normal conditions arise from both spike-dependent and -independent processes, and probably rely on the release of GABA from the synaptic terminals of inhibitory neurones which then interacts with $GABA_A$ receptors on layer V cells.

The time-to-peak of spontaneous fast inhibitory potentials was typically 1–5 ms measured at −60 mV, but as shown in Fig. 1*B*, hyperpolarizing events with longer times-to-peak were sometimes observed. The mean time-to-peak in the example was 2·6 ± 1·3 ms ($n = 219$). The rise time of a synaptic potential is dependent on its electrotonic distance from the recording site (Rall, 1967), so it seems plausible that inhibitory synapses are made at several different locations on the soma and dendritic processes of each neurone. Moreover, the finding that many inhibitory synaptic contacts are made on the cell bodies of layer V pyramidal neurones (for a review see White, 1989) suggests that the synapses providing the fastest rising IPSPs were present at, or very close to, the soma. The amplitude of spontaneous fast IPSPs discernable above the level of the noise of the recording system (0·2–0·4 mV) ranged upwards to a maximum of −2·4 mV (measured typically at −60 mV). The amplitudes for spontaneous fast IPSPs for one neurone are presented in Fig. 1*C*. The mean amplitude

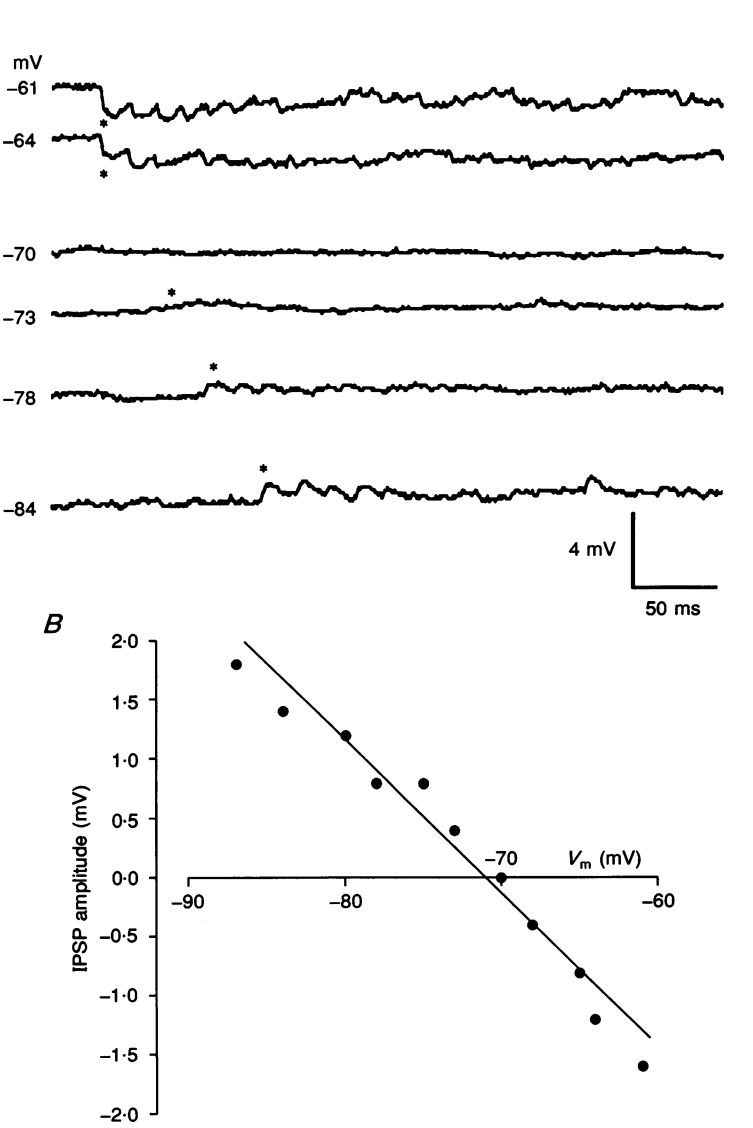

Figure 3. Determination of reversal potential and peak conductance change for glutamate-elicited fast IPSPs
Glutamate ejection adjusted to trigger a train of IPSPs for easier identification. *A*, IPSPs triggered at six different membrane potentials, as indicated. Events measured are marked with an asterisk. *B*, the peak amplitude of individual IPSPs plotted against membrane potential (V_m). A straight line fitted by linear regression analysis indicated that the IPSP reversed at approximately −71 mV. The slope of the straight line, 0·128, and the input resistance, 23 MΩ, gave a value of 6·4 nS for the peak conductance change due to this IPSP. Glutamate microapplications (5 mM) were made in the presence of CNQX (5 μM) and CPP (10 μM).

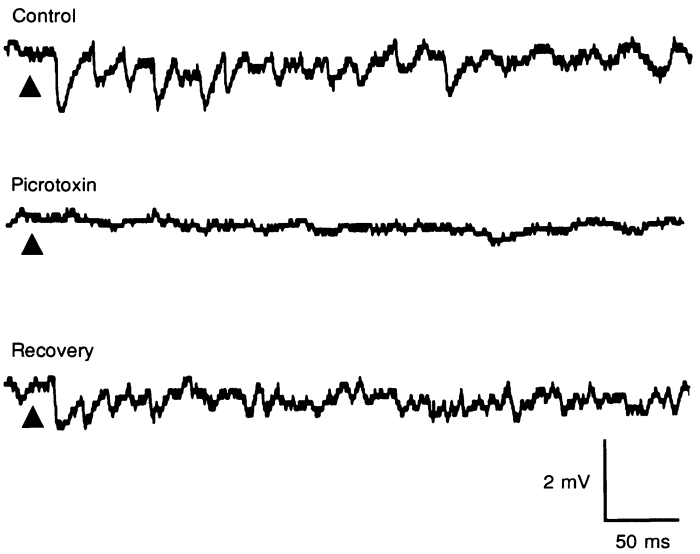

Figure 4. Fast IPSPs triggered by glutamate microapplication are mediated by $GABA_A$ receptors
IPSPs evoked by glutamate (2·5 mM) delivery (indicated at triangle) in *A*, were suppressed by the subsequent addition of picrotoxin (100 μM) in *B*, in a reversible manner (*C*). Membrane potential was maintained at −60 mV. Glutamate microapplications were made in the presence of CNQX (5 μM) and CPP (10 μM).

of these events in this cell was $-1{\cdot}0 \pm 0{\cdot}3$ mV (range −0·4 to −1·6 mV, $n = 219$), measured when the membrane potential was maintained at −60 mV.

Experiments were undertaken to explore the properties of the local inhibitory circuit in greater detail. This was accomplished by selectively stimulating local interneurones with glutamate microapplication, which in turn elicited IPSPs in layer V neurones. A detailed analysis of glutamate-evoked IPSPs was performed for forty-nine separate sites of application made while recording from a total of thirty-eight cells. In forty-two of these cases glutamate microapplication resulted in single or multiple discrete IPSPs having fast times-to-peak and short duration (e.g. Fig. 2*A* and *C*). A composite diagram showing the locations found to yield such IPSPs, relative to the recording sites in layer V is presented in Fig. 2*B*. The mean time-to-peak of these events for one neurone at a single site of glutamate microapplication was $2{\cdot}1 \pm 0{\cdot}6$ ms ($n = 162$; Fig. 2*D*). The mean IPSP amplitude for this example, measured at −60 mV was $-0{\cdot}9 \pm 0{\cdot}3$ mV (range, −0·4 to −1·6 mV; $n = 162$). The distribution of these amplitudes is shown in Fig. 2*E*. The mean time-to-peak for fast IPSPs for all the sites sampled was $2{\cdot}5 \pm 1{\cdot}1$ ms ($n = 42$). The mean peak amplitude of IPSPs measured at −60 mV, was $-1{\cdot}5 \pm 0{\cdot}4$ mV ($n = 42$). For these data, only non-overlapping IPSPs were measured (e.g. those marked with an asterisk in Figs 2*C* and 3*A*). The decay phase of the IPSP was fitted by a first power, single exponential

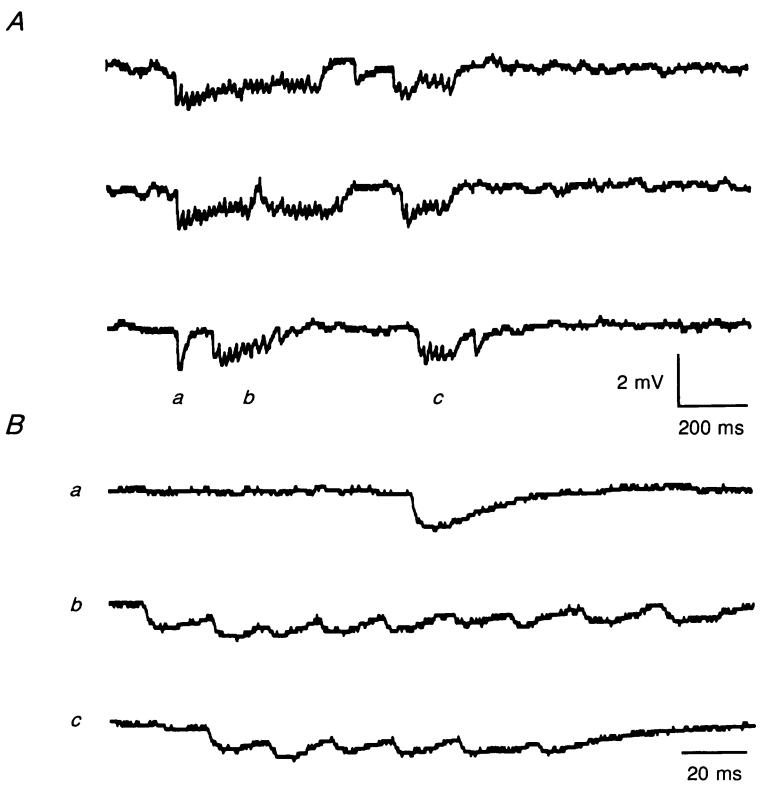

Figure 5. Glutamate microapplications could trigger bursts of fast IPSPs in layer V neurones
A, three responses to 15 ms pulses of glutamate (5 mM). *B*, (*a*, *b*, *c*), expanded sweeps of events designated *a*–*c* in lower trace in *A*, showing events are composed of bursts of individual fast IPSPs. Membrane potential was maintained at −60 mV. Glutamate microapplications were made in the presence of CNQX (5 μM) and CPP (10 μM).

function with a time constant of decay of $16{\cdot}4 \pm 6{\cdot}5$ ms ($n = 12$). For comparison, analysis of averaged voltage responses to hyperpolarizing current pulses in these cells showed the resultant charging curves were best fitted by a double exponential giving membrane time constants of $0{\cdot}50 \pm 0{\cdot}76$ ms and $7{\cdot}68 \pm 3{\cdot}51$ ms ($n = 12$).

For the cell in Fig. 3 the IPSPs reversed monotonically throughout their time course (Fig. 3*A*) at a membrane potential of -71 mV determined from the regression line of a plot of IPSP amplitude against membrane potential (Fig. 3*B*). The mean reversal potential for IPSPs was $-69{\cdot}3 \pm 2{\cdot}4$ mV (range -64 to -73 mV, $n = 42$). The peak IPSP conductance, g_{IPSP}, was obtained using the following relationship derived from that of Ginsborg (1973):

$$\frac{1}{g_{IPSP}} = R_n\left(\frac{E_{IPSP} - V_m}{V_{IPSP}}\right) - 1,$$

where R_n is the input resistance of the neurone, E_{IPSP} is the reversal potential for the IPSP, V_m is the membrane potential and V_{IPSP} the peak amplitude of the IPSP. Using direct measurements of R_n and values of $(E_{IPSP} - V_m)/V_{IPSP}$ derived from the slope of plots such as that of Fig. 3*B*, the peak synaptic conductance for the example was calculated to be 6·4 nS. The mean peak conductance for fast IPSPs was $9{\cdot}8 \pm 2{\cdot}9$ nS (range, 3·4–15·6 nS; $n = 42$).

The reversal potential and time course of these glutamate-evoked IPSPs suggested they were fast IPSPs mediated by $GABA_A$ receptors. This hypothesis was confirmed by application of the $GABA_A$ antagonist picrotoxin. Local application of picrotoxin (100 μM) via a separately manipulated micropipette completely suppressed all fast IPSPs elicited by glutamate microapplication for all ($n = 5$) inhibitory connections tested (Fig. 4), and did not uncover any underlying slow IPSPs. Therefore, variations in IPSP amplitude do not appear to rely on differences in postsynaptic receptors.

At or above the threshold for eliciting IPSPs, multiple events were often generated, usually with recognizable burst-like patterns (Fig. 5*A*). Detailed analysis of these IPSP bursts showed that each burst was actually composed of multiple discrete IPSPs (Fig. 5*Ba–c*). Initially the burst of hyperpolarizing events summated to amplitudes of up to 6 mV, measured at -60 mV. Later within the train of glutamate-triggered IPSPs, higher frequency events were noted, which did not appear to sum in the same manner, perhaps indicating depression of these events at faster frequencies of firing. Quantification of burst characteristics was difficult, because burst duration and composition could be variable, as shown in Fig. 5*A*. IPSP bursts (i.e. well-defined envelopes of hyperpolarization composed of individual fast IPSPs) averaged up to 346 ± 179 ms ($n = 13$). In general, increasing the duration of glutamate application gave longer duration IPSP bursts, but in response to longer applications (tens of milliseconds) the IPSP pattern became less organized, being more consistent with repetitive firing. IPSP frequencies achieved during bursts ranged between 50 and 500 Hz (mean, 183 ± 117 Hz; $n = 13$), though it was often quite difficult to resolve IPSP frequencies above 250 Hz.

IPSP bursts have previously been noted in hippocampus (Miles & Wong, 1984), where such patterns of IPSPs are known to be initiated by bursts of action potentials in presynaptic inhibitory neurones. In the present experiments, where IPSPs are triggered by glutamate application, burst-like patterns of IPSPs may represent a fortuitous temporal patterning of the activity of several inhibitory cells, or more probably could depend on inhibitory neurones firing in bursts of action potentials, similar to the situation encountered in hippocampus.

Comparison of the properties of the population fast IPSP evoked by afferent stimulation with glutamate-triggered fast IPSPs

Next, the properties of glutamate-induced fast IPSPs, evoked when many if not all inhibitory synapses onto a single cell are synchronously fired (i.e. the population IPSP), were compared with those of maximally activated IPSPs. Unfortunately, it would be impossible to activate neocortical inhibitory synapses with electrical stimulation without simultaneously activating other synapses. In neocortical neurones temporal overlap of the various evoked synaptic potentials even further complicates such comparison. Because the time course of the NMDA component of the EPSP overlaps the fast IPSP, there is significant obscuration of the electrically evoked fast synaptic hyperpolarization (Benardo, 1993*b*). Since this potential is taken as an indication of the fast IPSP, this would lead to distortions of reversal potential and conductance measurements when moderate to high intensity stimuli are used. I have observed that application of an NMDA antagonist unmasks the underlying IPSP without affecting its magnitude (Benardo, 1993*b*), thus allowing more accurate measures of reversal potential and conductance. Accordingly, layer V neurones were bathed in control solution to which the NMDA antagonist CPP (10 μM) was added, and stimulated at an intensity yielding maximal fast IPSPs. Concurrently, glutamate micro-applications were made at selected sites on these same cells ($n = 7$), allowing comparison of these potentials with those of the population IPSP. The results are shown in Fig. 6.

The time period from the onset of the population IPSP to its peak ranged from 5 to 15 ms. The total duration of the population IPSP could not be measured due to the presence of the slow IPSP (though with submaximal stimulation it appeared to last 40–70 ms). The peak amplitude for the population IPSP was $-5{\cdot}5 \pm 1{\cdot}2$ mV

(range, −3·6 to −7·0 mV; $n = 7$) measured at −60 mV (e.g. Fig. 6*A*). The peak amplitude for glutamate-evoked IPSPs in these same cells was −1·8 ± 0·5 mV (range, −0·8 to −2·2 mV), at the same membrane potential (e.g. Fig. 6*C*). The reversal potential for the population IPSP was −71·0 ± 2·8 mV, which was in good agreement with that of glutamate-induced IPSPs, i.e. −70·5 ± 2·5 mV (cf. Fig. 6*B* and *D*). The mean peak conductance for the population IPSP was 65·0 ± 36·5 nS (range, 29·8–116·9 nS), while that for glutamate-evoked IPSPs in these same neurones was 12·2 ± 3·1 nS (range, 6·0–15·3 nS).

Properties of slow inhibitory synaptic potentials

In seven attempts glutamate microapplication triggered IPSPs in layer V cells which appeared qualitatively and quantitatively different from those described above (e.g. Fig. 7*A*). For example, times-to-peak were at least 10 ms (mean, 45 ± 23 ms, range, 10–120 ms; $n = 7$), amplitudes measured at −60 mV had a mean of −4·4 ± 3·4 mV (range, −0·8 to −10 mV; $n = 7$), and the duration of these events was 200–1600 ms (mean, 973 ± 420 ms; $n = 7$). Variability in

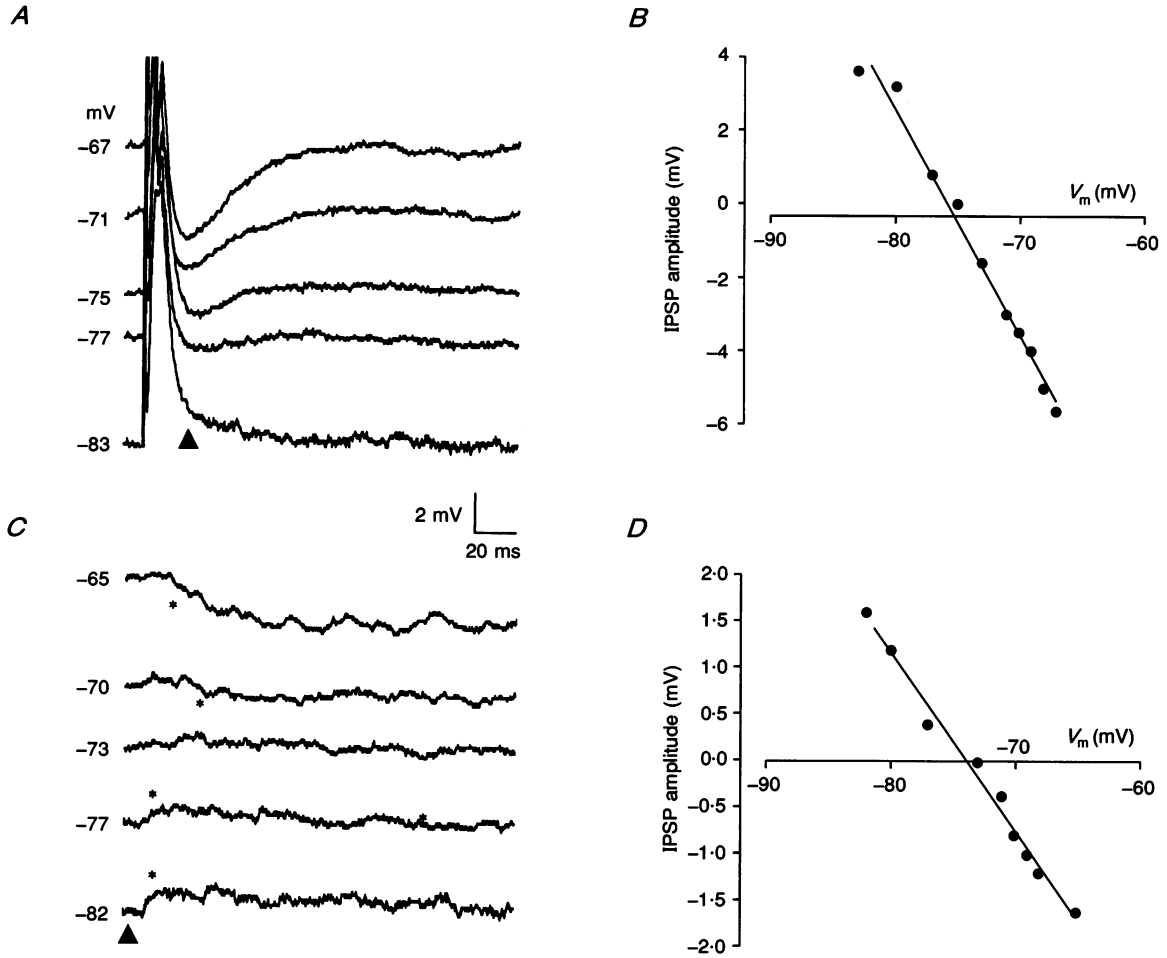

Figure 6. Voltage dependence of the population IPSP compared with that of the glutamate-triggered IPSP

A, responses at five membrane potentials to electrical stimulation in layer VI, adjusted to elicit the maximal IPSP. The peak fast IPSP amplitudes derived at the points indicated by the triangle in *A* are plotted against membrane potential (V_m) in *B*. *C*, glutamate-evoked (2·5 mM) IPSPs in the same cell, triggered at five different membrane potentials, as indicated. The triangle marks the offset of a 10 ms application of 2·5 mM glutamate. Events measured are marked with an asterisk. *D*, the peak amplitude of individual IPSPs in *C* plotted against membrane potential (V_m). Straight lines fitted by linear regression analysis indicated that the population IPSP reversed at approximately −75 mV (*B*), while the glutamate-triggered IPSPs reversed at approximately −74 mV (*D*). The slope of the straight lines (6·1 and 0·189, for *B* and *D*, respectively), and the input resistance, 16 MΩ, gave a value of 97 nS for the peak conductance of the population IPSP, and a value of 14·5 nS for the peak glutamate-evoked IPSP in this cell. The bathing medium was of physiological composition except that it contained CPP (10 μM), to insure the fast population IPSP would not be obscured by the overlapping NMDA component of the EPSP (see text).

slow IPSP parameters was seen within single cells. For one neurone the mean time-to-peak of the IPSP was 48 ± 25 ms (range, 22–100 ms; $n = 20$). The mean amplitude recorded at −60 mV was −2·3 ± 1·0 mV (range, −0·8 to −4·8 mV; $n = 20$). IPSP duration averaged 857 ± 336 ms (range, 300–1600 ms; $n = 20$). It was more difficult to localize sites giving these potentials. In all cases the sites providing these types of IPSPs were located within a region approximately 50–100 μm ventral to the recording sites (with a radius of about 50 μm; Fig. 7*D*). No discernible differences were noted between cells in which slow IPSPs were elicited *versus* those in which fast IPSPs were triggered. Moreover, in three cells showing slow IPSPs, fast IPSPs were also seen, though they were generated from different sites.

The best evidence that these IPSPs were distinct from the chloride-mediated $GABA_A$ IPSPs previously encountered, was the disparate reversal potential (Fig. 7*A* and *B*), and the fact that in four of the seven cases, recordings were made with KCl-filled microelectrodes. In these instances chloride-mediated events are depolarizing at −60 mV (e.g. Fig. 7*C*; Thompson, Deisz & Prince, 1988), due to a positive shift in the chloride reversal potential. But the slow IPSPs elicited by glutamate microapplication remained hyperpolarizing. In two cells recorded with KCl electrodes fast depolarizing IPSPs had previously been elicited (Fig. 7*C*), again from different stimulation sites. Moreover, in cells recorded with KCl electrodes, picrotoxin-sensitive hyperpolarizing IPSPs were never seen.

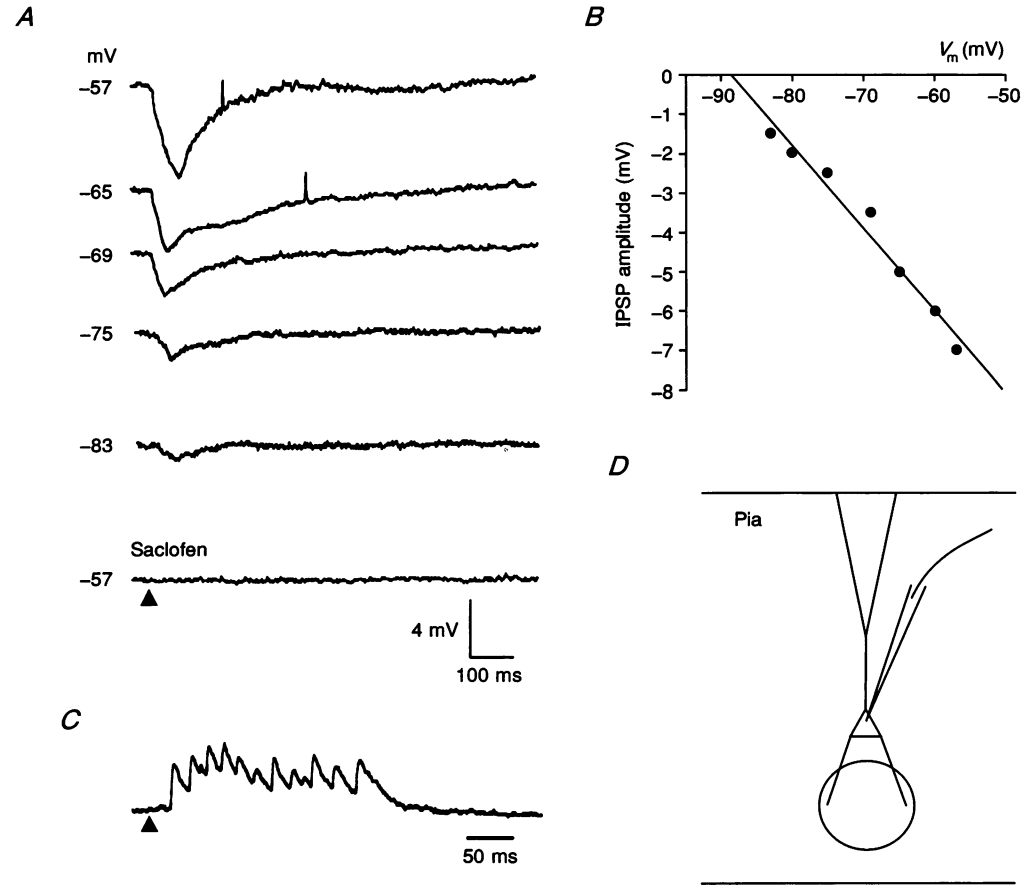

Figure 7. Slow IPSPs evoked in layer V neurones by glutamate microapplication
A, responses to glutamate micro-delivery were characterized by their slow time-to-peak and long duration (here shown at five different membrane potentials). The glutamate-evoked slow IPSP was suppressed by the addition of 2-hydroxysaclofen (0·5 mM), suggesting it was mediated by $GABA_B$ receptors. *B*, the peak amplitude of individual IPSPs from same cell as in *A*, plotted against membrane potential (V_m). The straight line fitted by linear regression analysis indicated a reversal potential of about −88 mV. The slope of the straight line, 0·21, and the input resistance, 23 MΩ, gave a value of 11·6 nS for the peak conductance of this IPSP. *C*, fast IPSPs recorded using KCl-filled electrodes were depolarizing when recorded at −60 mV, but slow IPSPs recorded with these same electrodes remained hyperpolarizing. Slow IPSPs were only triggered when glutamate was delivered within a specific region relative to the recording site, as indicated by the encircled area in *D*. Membrane potentials throughout were maintained at −60 mV and glutamate microapplications were made in the presence of CNQX (5 μM) and CPP (10 μM). Triangles mark the offset of a 30 ms application of 2·5 mM glutamate.

The slow IPSPs evoked by glutamate microapplication had a mean reversal potential of $-89{\cdot}2 \pm 5{\cdot}0$ mV (range, -82 to -97; $n = 7$) when calculated from plots of IPSP amplitude against membrane potential (e.g. -88 mV in Fig. 7*B*). Taken together the data suggested that these events were slow, potassium-dependent IPSPs. Peak conductances were obtained using the same procedure described earlier for fast IPSPs. In the example in Fig. 7*B*, the slope of the regression was 0·21 and R_n was 23 MΩ, giving a peak conductance of 11·6 nS. The mean peak conductance was $7{\cdot}7 \pm 4{\cdot}9$ nS (range, 3·6–16·8 nS; $n = 7$).

At sites yielding fast IPSPs, suprathreshold amounts of glutamate often gave multiple summating individual IPSPs. For slow IPSPs supramaximal glutamate microapplications could give larger slow inhibitory events, but it was not clear that these potentials were composed of discrete slow IPSP components. Rather, both large and small hyperpolarizations presented smooth rising phases throughout the course of these potentials.

Verification of the pharmacological identity of these potentials was carried out in one case as shown in Fig. 7*A* (lower trace). Here 2-hydroxysaclofen (0·5 mM) delivered from a separately manipulated micropipette effectively blocked the slow IPSP elicited by glutamate microapplication, suggesting that this IPSP did indeed arise from interaction of GABA at $GABA_B$ receptors.

DISCUSSION

In this report synaptic inhibition in layer V neurones from somatosensory cortex was studied by stimulating inhibitory neurones using glutamate microapplication. By this approach reversal potential and conductance values were derived for these IPSPs. On the basis of reversal potential the responses could be characterized as either chloride-mediated or potassium-dependent events, and mixed potentials were never seen. The majority of sites yielding IPSPs in layer V cells triggered fast, chloride-mediated, $GABA_A$-type potentials. Less frequently, glutamate delivery elicited slow, potassium-mediated, $GABA_B$-type IPSPs, identifying another group of neocortical inhibitory neurones.

Properties of fast chloride-mediated IPSPs

An important issue in considering the present results is whether the glutamate-triggered fast IPSPs encountered here were indeed unitary IPSPs. By utilizing concentrations of glutamate antagonists which are effective in blocking evoked glutamatergic transmission, polysynaptic excitation should be eliminated. It is clear that IPSPs generated by glutamate microapplication did exhibit considerable fluctuations in amplitude, and that the amplitudes of individual IPSPs were much smaller than those of evoked population IPSPs. Moreover, the range of amplitude fluctuations remained unchanged when the stimulation by glutamate was increased. The amount of fluctuation was similar to that seen with spontaneously occurring IPSPs. Nevertheless, the possibility that glutamate interacted with more than one inhibitory neurone, each of which in turn formed synapses on the recorded cell, cannot be ruled out at present. Glutamate-evoked fast IPSPs did not always have a fixed latency from the onset of equivalent glutamate ejections. Whether this arose from excitation of differing numbers of inhibitory neurones with each glutamate pulse, or from excitation of a single inhibitory cell in which the physiological state (e.g. the membrane potential) changed between each ejection, cannot be discerned at this time. Thus, it remains equivocal whether all the fast IPSPs evoked in the present experiments represent unitary events.

A detailed study of evoked unitary fast IPSPs in neocortex has not been performed previously (but see the elegant study employing paired recordings of neocortical neurones by Thomson, Deuchars & West, 1993, who identified three cases in which IPSPs in one neurone were triggered by excitation of a second cell). In fact, only a handful of reports have described unitary events at inhibitory synapses in mammalian central neurones (Jankowska & Roberts, 1972; Kuno & Weakly, 1972; Miles & Wong, 1984; Edwards, Konnerth & Sakmann, 1990; Takahashi, 1992). Only one of these reports examined such events in pyramidal-type neurones in a cortical area. Miles & Wong (1984) specified the properties of chloride-mediated fast IPSPs in CA3 hippocampal pyramidal neurones using dual intracellular recordings. Many of the properties of unitary fast IPSPs which they described are similar to those of the glutamate-evoked IPSPs uncovered in my experiments. They found such events to range between $-1{\cdot}3$ and $-3{\cdot}1$ mV at postsynaptic potentials between -60 and -70 mV. In the present study, fast IPSPs measured at -60 mV had a mean amplitude of $-1{\cdot}5 \pm 0{\cdot}4$ mV, and ranged up to $-2{\cdot}4$ mV. In general, their IPSPs had slightly higher amplitudes, and a wider range than those encountered in neocortex. In part, this may be due to differences in neuronal input resistance, with that of CA3 pyramidal neurones being 20–40 MΩ (Miles & Wong, 1984) as compared to 15–30 MΩ in layer V cells (this study; Benardo, 1993*a*, *b*). The conductance change underlying IPSPs contributes significantly to their amplitude. In hippocampus the mean peak conductance for fast IPSPs was 6·7 nS, compared to 9·8 nS in the present study. Thus, while the amplitudes of IPSPs in neocortex were somewhat smaller than those recorded in hippocampus, neocortical IPSPs were associated with somewhat higher peak conductances.

Comparison of glutamate-evoked fast IPSPs with the population IPSP was undertaken to examine whether these IPSPs were indeed generated by similar mechanisms. The finding of similar reversal potentials, and the observation that both were blocked by picrotoxin was convincing evidence that the same neurotransmitter, GABA, via $GABA_A$ receptor activation, was responsible for both events. Glutamate-evoked and population IPSPs

had disparate times-to-peak, with the population IPSP having the slower time-to-peak. This probably arose from temporal overlap with the EPSP. The finding that glutamate microapplication elicited bursts of IPSPs suggests that similar bursts may accompany electrically evoked population IPSPs. This would be expected to give rise to prolonged population IPSPs, especially when feedforward excitation is enhanced.

The amplitude of the population IPSP is influenced by the number of inhibitory neurones which synapse onto a cell and are activated by a stimulus. This number may be estimated by comparing the conductance change associated with unitary IPSPs with that for the population IPSP. The mean value for the conductance change of glutamate-evoked IPSPs was 9·8 nS, and the largest value for the evoked population IPSP was 116 nS (cf. mean values of 72 nS in Connors *et al.* 1988, and 193 nS in Deisz & Prince, 1989, in layer II–III cells calculated using a different method). Thus, if we accept that glutamate-triggered fast IPSPs are indeed unitary events, it appears that at least eleven inhibitory neurones make synapses onto a particular layer V neurone. It is likely that this number is an underestimate of that present in the intact neocortex.

Properties of slow potassium-mediated IPSPs

Slow potassium-dependent IPSPs mediated by GABA acting at $GABA_B$ receptors are now accepted as one of the typical responses to afferent stimulation in the neocortex. It was unknown whether such potentials could be triggered in isolation in neocortex, though this had been demonstrated in hippocampus (Segal, 1987, 1990; Lacaille & Schwartzkroin, 1988; Williams & Lacaille, 1992). The present results show that slow potassium-mediated IPSPs may be triggered alone using glutamate microapplication. Presumably this results from glutamate exciting inhibitory neurones which in turn innervate only $GABA_B$ receptors in the recorded postsynaptic layer V cell. It remains unclear whether these cells innervate $GABA_A$ receptors on other cells. Regardless, these results suggest a high degree of organization within local inhibitory circuits, including pharmacological specificity of afferents.

Several other interesting features of this circuit are suggested by these findings. For example, sites giving rise to slow IPSPs were found far less frequently than those giving rise to fast IPSPs (i.e. with a ratio of 1 to 6). The time-to-peak of the slow IPSPs was variable, but generally was much slower than that of the fast IPSPs. In addition, these potentials were associated with a wider range of conductance values (i.e. 3·6–16·8 nS). The mean peak conductance for slow IPSPs calculated here was 7·7 nS, similar to that derived for fast IPSPs. Interestingly, the population slow IPSP calculated in previous studies was 10–20 nS (Connors *et al.* 1988; Deisz & Prince, 1989). If the events triggered by glutamate are unitary, it would appear that only a few inhibitory interneurones contribute to the population slow IPSP. Alternatively, inhibitory interneurones mediating slow IPSPs may be arranged in clusters so that glutamate application excites more than one cell, all of which in turn synapse onto the recorded neurone. Another possibility is that these inhibitory cells are electrotonically coupled to others giving rise to $GABA_B$ IPSPs (Michelson & Wong, 1991). In this way large slow IPSPs result if either these coupled cells all make synapses on the recorded layer V neurone, or there is reverberating activity occurring within the inhibitory network.

Implications for segregated $GABA_A$ and $GABA_B$ IPSPs

Previous considerations of inhibitory neurones tended to group them all into a single class of neurone which was GABAergic, and had a distinct physiology (Knowles & Schwartzkroin, 1981; McCormick *et al.* 1985). Results from additional studies in hippocampus (Miles & Wong, 1984; Lacaille *et al.* 1987; Kawaguchi & Hama, 1987, 1988; Kunkel, Lacaille & Schwartzkroin, 1988; Lacaille & Schwartzkroin, 1988) and neocortex (Kawaguchi, 1993) would seem to argue against this notion, suggesting there are different interneuronal populations. The precise roles of different interneuronal populations remains to be fully elucidated.

The emerging evidence from studies in hippocampus (Miles & Wong, 1984; Lacaille *et al.* 1987; Lacaille & Schwartzkroin, 1988), lateral amygdala and ventral tegmental area (Sugita, Johnson & North, 1992), and thalamus (Steriade, Deschenes, Domich & Mulle, 1985; Crunelli & Leresche, 1991) suggests that different populations of interneurones account for separate activation of fast and slow inhibition, and that different classes of interneurones may actually synapse with only $GABA_A$ or $GABA_B$ receptors (see also Benardo & Wong, 1994, for review). Nonetheless an alternative hypothesis still remains (Isaacson, Solis & Nicoll, 1993), namely that GABA is released from single interneurones to act primarily with $GABA_A$ receptors, but with greater release (e.g. with higher levels of stimulation: Dutar & Nicoll, 1988), or depressed transmitter uptake (Isaacson *et al.* 1993), GABA can 'spillover' onto $GABA_B$ receptors, which are postulated to have a more diffuse distribution. My finding that fast and slow IPSPs are separately triggered in the neocortex, suggests the former type of organization may be present in this structure, i.e. there are two populations of inhibitory neurones, which individually are responsible for fast and slow inhibition. The organization of outputs of two separate populations of GABAergic inhibitory neurones may be quite different (cf. Schwartzkroin & Mathers, 1978; Knowles & Schwartzkroin, 1981; Steriade *et al.* 1985; Lacaille *et al.* 1987; Lacaille & Schwartzkroin, 1988; Crunelli & Leresche, 1991; Sugita *et al.* 1992). Moreover, if fast and slow inhibition arise from two separate cell populations, there is the possibility that these two types of GABAergic inhibition can be independently modulated both at presynaptic, as well as postsynaptic sites.

REFERENCES

ALGER, B. E. (1991). Gating of GABAergic inhibition in hippocampal pyramidal cells. In *Activity Driven CNS Changes in Learning and Development*, ed. WOLPAW, J. R., SCHMIDT, J. T. & VAUGHN, T. M., pp. 249–263. New York Academy of Sciences, New York.

AVOLI, M. (1986). Inhibitory potentials in neurons of the deep layers of the in vitro neocortical slice. *Brain Research* **370**, 165–170.

BENARDO, L. S. (1991). Acetylcholine and norepinephrine mediate slow synaptic potentials in normal and epileptic neocortex. *Neuroscience Letters* **126**, 137–140.

BENARDO, L. S. (1993*a*). Characterization of cholinergic and noradrenergic slow excitatory post-synaptic potentials from rat cerebral cortical neurons. *Neuroscience* **53**, 11–22.

BENARDO, L. S. (1993*b*). Recruitment of inhibition by enhanced activation of synaptic NMDA responses in the rat cerebral cortex. *Brain Research* **627**, 314–324.

BENARDO, L. S. & WONG, R. K. S. (1994). Inhibition in the cortical network. In *Normal and Pathological Physiology of the Cortical Neuron*, ed. MODY, I. & GUTNICK, M. J. Oxford University Press, New York.

BISCOE, T. J. & CURTIS, D. R. (1967). Strychnine and cortical inhibition. *Nature* **214**, 914–915.

BRINK, E., HARRISON, P. J., JANKOWSKA, E., MCCREA, D. A. & SKOOG, B. (1983). Post-synaptic potentials in a population of motoneurones following activity of single interneurones in the cat. *Journal of Physiology* **343**, 341–359.

CHAGNAC-AMITAI, Y. & CONNORS, B. W. (1989). Horizontal spread of synchronized activity in neocortex and its control by GABA-mediated inhibition. *Journal of Neurophysiology* **61**, 747–758.

CHRISTIAN, E. P. & DUDEK, F. E. (1988). Characteristics of local excitatory circuits studied with glutamate microapplication in the CA3 area of rat hippocampal slices. *Journal of Neurophysiology* **59**, 90–109.

CONNORS, B. W. (1984). Initiation of synchronized neuronal bursting in neocortex. *Nature* **310**, 685–687.

CONNORS, B. W., GUTNICK, M. J. & PRINCE, D. A. (1982). Electrophysiological properties of neocortical neurons *in vitro*. *Journal of Neurophysiology* **48**, 1302–1320.

CONNORS, B. W., MALENKA, R. C. & SILVA, L. R. (1988). Two inhibitory postsynaptic potentials, and $GABA_A$ and $GABA_B$ receptor-mediated responses in neocortex of rat and cat. *Journal of Physiology* **406**, 443–468.

CRAWFORD, J. M., CURTIS, D. R., VOORHOEVE, P. E. & WILSON, V. J. (1966). Acetylcholine sensitivity of cerebellar neurones in the cat. *Journal of Physiology* **186**, 139–165.

CRUNELLI, V. & LERESCHE, N. (1991). A role for $GABA_B$ receptors in excitation and inhibition at thalamocortical cells. *Trends in Neurosciences* **14**, 16–21.

CURTIS, D. R. & CRAWFORD, J. M. (1965). Acetylcholine sensitivity of cerebellar neurones. *Nature* **206**, 516–517.

CURTIS, D. R. & FELIX, D. (1971). The effect of bicuculline upon synaptic inhibition in the cerebral and cerebellar cortices of the cat. *Brain Research* **34**, 301–321.

DEISZ, R. A. & PRINCE, D. A. (1989). Frequency-dependent depression of inhibition in guinea-pig neocortex *in vitro* by $GABA_B$ receptor feed-back on GABA release. *Journal of Physiology* **412**, 513–541.

DREJER, T. & HONORE, T. (1988). New quinoxalinediones show potent antagonism of quisqualate responses in cultured mouse cortical neurons. *Neuroscience Letters* **87**, 104–108.

DUTAR, P. & NICOLL, R. A. (1988). A physiological role for $GABA_B$ receptors in the central nervous system. *Nature* **332**, 156–158.

EDWARDS, F. A., KONNERTH, A. & SAKMANN, B. (1990). Quantal analysis of inhibitory synaptic transmission in the dentate gyrus of rat hippocampal slices: a patch-clamp study. *Journal of Physiology* **430**, 213–249.

GINSBORG, B. L. (1973). Electrical changes in the membrane in junctional transmission. *Biochimica et Biophysica Acta* **300**, 289–317.

HOWE, J. R., SUTOR, B. & ZIEGLGANSBERGER, W. (1987). Baclofen reduces post-synaptic potentials of rat cortical neurones by an action other than its hyperpolarizing action. *Journal of Physiology* **384**, 539–569.

ISAACSON, J., SOLIS, J. M. & NICOLL, R. A. (1993). Local and diffuse synaptic actions of GABA in the hippocampus. *Neuron* **10**, 165–175.

JANKOWSKA, E. & ROBERTS, W. J. (1972). Synaptic actions of single interneurones mediating reciprocal Ia inhibition of moto-neurones. *Journal of Physiology* **222**, 623–642.

KAWAGUCHI, Y. (1993). Groupings of nonpyramidal and pyramidal cells with specific physiological and morphological characteristics in rat frontal cortex. *Journal of Neurophysiology* **69**, 416–431.

KAWAGUCHI, Y. & HAMA, K. (1987). Two subtypes of nonpyramidal cells in rat hippocampal formation identified by intracellular recording and HRP injection. *Brain Research* **411**, 190–195.

KAWAGUCHI, Y. & HAMA, K. (1988). Physiological heterogeneity of nonpyramidal cells in rat hippocampal CA1 region. *Experimental Brain Research* **72**, 494–502.

KELLY, J. S., KRNJEVIC, K., MORRIS, M. E. & YIM, G. K. W. (1969). Anionic permeability of cortical neurones. *Experimental Brain Research* **7**, 11–31.

KNOWLES, W. D. & SCHWARTZKROIN, P. A. (1981). Local circuit synaptic interactions in hippocampal brain slices. *Journal of Neuroscience* **1**, 318–322.

KRNJEVIC, K. (1984). Neurotransmitters in cerebral cortex: A general account. In *Cerebral Cortex*, vol. 2., *Functional Properties of Cortical Cells*, ed. JONES, E. G. & PETERS, A., pp. 39–62. Plenum Press, New York.

KUNKEL, D. D., LACAILLE, J.-C. & SCHWARTZKROIN, P. A. (1988). Ultrastructure of stratum lacunosum-moleculare interneurons of hippocampal CA1 region. *Synapse* **2**, 382–394.

KUNO, M. & WEAKLY, J. N. (1972). Quantal components of the inhibitory synaptic potential in spinal motoneurones of the cat. *Journal of Physiology* **224**, 287–303.

LACAILLE, J.-C., MUELLER, A. L., KUNKEL, D. D. & SCHWARTZKROIN, P. A. (1987). Local circuit interactions between oriens/alveus interneurons and CA1 pyramidal cells in hippocampal slices: Electrophysiology and morphology. *Journal of Neuroscience* **7**, 1979–1993.

LACAILLE, J.-C. & SCHWARTZKROIN, P. A. (1988). Stratum lacunosum-moleculare interneurons of hippocampal CA1 region. I. Intracellular response characteristics, synaptic responses, and morphology. *Journal of Neuroscience* **8**, 1400–1410.

MCCORMICK, D. A. (1989). GABA as an inhibitory neurotransmitter in human cerebral cortex. *Journal of Neurophysiology* **62**, 1018–1027.

MCCORMICK, D. A., CONNORS, B. W., LIGHTHALL, J. W. & PRINCE, D. A. (1985). Comparative physiology of pyramidal and sparsely spiny neurons of the neocortex. *Journal of Neurophysiology* **54**, 782–806.

MICHELSON, H. B. & WONG, R. K. S. (1991). Excitatory synaptic responses mediated by $GABA_A$ receptors in the hippocampus. *Science* **253**, 1420–1423.

MILES, R. (1990). Synaptic excitation of inhibitory cells by single CA3 hippocampal pyramidal cells of the guinea-pig *in vitro*. *Journal of Physiology* **428**, 61–77.

MILES, R. & WONG, R. K. S. (1984). Unitary inhibitory synaptic potentials in the guinea-pig hippocampus *in vitro*. *Journal of Physiology* **356**, 97–113.

MILES, R. & WONG, R. K. S. (1986). Excitatory synaptic interactions between CA3 neurones in the guinea-pig hippocampus *in vitro*. *Journal of Physiology* **373**, 397–418.

RALL, W. (1967). Distinguishing theoretical synaptic potentials computed for different soma-dendritic distributions of synaptic input. *Journal of Neurophysiology* **30**, 1138–1168.

RENAUD, L. P. & KELLY, J. S. (1974). Identification of possible inhibitory neurons in the pericruciate cortex of the cat. *Brain Research* **79**, 9–28.

SCHWARTZKROIN, P. A. & MATHERS, L. H. (1978). Physiological and morphological identification of a nonpyramidal hippocampal cell type. *Brain Research* **157**, 1–10.

SEGAL, M. (1987). Repetitive inhibitory postsynaptic potentials evoked by 4-aminopyridine in hippocampal neurons *in vitro*. *Brain Research* **414**, 285–293.

SEGAL, M. (1990). A subset of local interneurons generate slow inhibitory postsynaptic potentials in hippocampal neurons. *Brain Research* **511**, 163–164.

STERIADE, M., DESCHENES, M., DOMICH, L. & MULLE, C. (1985). Abolition of spindle oscillations in thalamic neurons disconnected from nucleus reticularis thalami. *Journal of Neurophysiology* **54**, 1473–1497.

SUGITA, S., JOHNSON, S. W. & NORTH, R. A. (1992). Synaptic inputs to $GABA_A$ and $GABA_B$ receptors originate from discrete afferent neurons. *Neuroscience Letters* **134**, 207–211.

TAKAHASHI, T. (1992). The minimal inhibitory synaptic currents evoked in neonatal rat motoneurones. *Journal of Physiology* **450**, 593–611.

TASKER, J. G., PEACOCK, W. J. & DUDEK, F. E. (1992). Local synaptic circuits and epileptiform activity in slices of neocortex from children with intractable epilepsy. *Journal of Neurophysiology* **67**, 496–507.

THOMPSON, S. M., DEISZ, R. A. & PRINCE, D. A. (1988). Relative contributions of passive equilibrium and active transport to the distribution of chloride in mammalian cortical neurons. *Journal of Neurophysiology* **60**, 105–124.

THOMSON, A. M., DEUCHARS, J. & WEST, D. C. (1993). Single axon excitatory postsynaptic potentials in neocortical interneurons exhibit pronounced paired pulse facilitation. *Neuroscience* **54**, 347–360.

TRAUB, R. D. & WONG, R. K. S. (1982). Cellular mechanism of neuronal synchronization in epilepsy. *Science* **216**, 745–747.

WATKINS, J. C. & OLVERMAN, H. J. (1987). Agonists and antagonists for excitatory amino acid receptors. *Trends in Neurosciences* **10**, 265–272.

WHITE, E. L. (1989). *Cortical Circuits. Synaptic Organization of the Cerebral Cortex. Structure, Function and Theory.* Birkhauser, Boston, MA, USA.

WILLIAMS, S. & LACAILLE, J.-C. (1992). $GABA_B$ receptor-mediated inhibitory postsynaptic potentials evoked by electrical stimulation and by glutamate stimulation of interneurons in stratum lacunosum-moleculare in hippocampal CA1 pyramidal cells *in vitro*. *Synapse* **11**, 249–258.

YAMAMOTO, C. (1982). Quantal analysis of excitatory postsynaptic potentials induced in hippocampal neurons by activation of granule cells. *Experimental Brain Research* **46**, 170–176.

Acknowledgements

I would like to thank Drs R. K. S. Wong and D. S. F. Ling for helpful discussions. This work was supported by a grant from the NIH (NS 01386).

Received 25 May 1993; revised 10 August 1993; accepted 14 September 1993.